applied sciences

MDPI

Article

Model-Based Fiber Diameter Determination Approach to Fine Particulate Matter Fraction ($PM_{2.5}$) Removal in HVAC Systems

Marlena Drąg

Department of Control Systems and Mechatronics, Wrocław University of Science and Technology, Wybrzeże Wyspiańskiego 27, 50-370 Wrocław, Poland; marlena.drag@pwr.edu.pl

Abstract: Particulate Matter (PM) is a general term to classify air pollutants consisting of airborne particles. The particles vary in composition and size, and the sizes of particles range from 2.5 µm ($PM_{2.5}$) to 10 µm (PM_{10}). Anthropogenic activity (e.g., industrial processes or fuel/waste combustion) stands as the main emission source of PM. Due to the fact that indoor PM penetrates from the outside to indoor air, Heating, Ventilation, and Air-Conditioning (HVAC) filtration systems may play a significant role in decreasing air pollution indoors. The section of the respiratory tract affected by particulate matter depends on the particle size. The smaller the fraction, the more deeply it can enter into lungs and bronchi, causing a series of health problems. Conventional electret air filters applied in HVAC systems are not able to efficiently remove $PM_{2.5}$ (e.g., huge gaps between thick fibers and unintentional elimination of electrostatic effects). The electrospinning process allows for the production of fibers of diverse diameters, including ultrathin yarns. The following work presents the axial length scale χ estimation method for the given conditions and experimental results. According to this approach, it is possible to find out what parameters should be used to produce materials at certain fiber diameters and to capture fine particulate matter fractions ($PM_{2.5}$). This research refers to poly(acrylonitrile) (PAN) fibers. The most important advantages, limitations, and challenges of the presented methodology are detected and discussed in this work.

Keywords: fine particulate matter ($PM_{2.5}$); electrospinning; air filtration; HVAC system; mathematical model; numerical optimization

Citation: Drąg, M. Model-Based Fiber Diameter Determination Approach to Fine Particulate Matter Fraction ($PM_{2.5}$) Removal in HVAC Systems. *Appl. Sci.* **2021**, *11*, 1014. https://doi.org/10.3390/app11031014

Received: 30 November 2020
Accepted: 20 January 2021
Published: 23 January 2021

1. Introduction

Nowadays, not everyone can breathe clean air [1]. The problem concerns mainly high urbanized [2] and industrialized [3] areas, where contamination levels significantly exceed the World Health Organization (WHO) guidelines and recommendations [4]. Studies indicate that people spend most of their time (≈90%) indoors [5]. In general, pollutants can get into human settlements through the filters assembled in the Heating, Ventilation and Air-Conditioning (HVAC) systems; the supply air can come entirely from the outside (European countries) or can be the mixture of the outside and recirculated air (USA) [6]. Even small amounts of pollutants can be dangerous due to long-term exposure [7].

The origin and characteristics of air pollution is varied and complex [8]. Particulate matter consists of both solid particles and liquid droplets, which are a mixture of organic and inorganic substances [9]. Two main fractions of particulate matter can be distinguished: (i) $PM_{2.5}$, which consists of compounds up to 2.5 µm in aerodynamic diameter, and (ii) PM_{10}, which consists of compounds up to 10 µm in aerodynamic diameter. The division due to fraction size is very important because, the smaller the dimensions of the PM, the greater the threat to the respiratory system [10]. Therefore, HVAC filters able to capture specified air contaminants are desirable for public health considerations [11].

The most popular solution refers to electret/charged filter media; several studies have addressed the role of such materials in HVAC systems. Tang et al. [12] explained how the applied approach can influence the particle separation efficiency. The study was subjected to typical commercial flat-sheet electret materials and particles of sizes of 3–500 nm. The results revealed that, depending on the particle size, different electrostatic mechanisms have different impacts on filtration enhancement; for particles of ≈20 nm, polarization force; for ≈100 nm, image force; and for ≈300 nm, Coulombic force. The filtration electret media produced by Cai et al. [13] was characterized by 99.96% filtration efficiency and low pressure drop (54 Pa). Li and coauthors [14] developed an electret membrane with 99.992% filtration efficiency and pressure drop of 61 Pa. Both types of membranes were tested against particles of 300 nm in size. Dust loading, particle size, or filter geometry can limit the filtration efficiency of the electret media. Thus, it is worth considering the worst-case scenario assuming a complete lack of charge. The common discharging standards are based on the fiber treatment with isopropanol liquid immersion or isopropanol saturated vapor [5,15]. Tang and coauthors [6] used a combination of electret and mechanical particle capture processes in their work. The developed filter consisted of commercial electret flat-sheet HVAC filter media and nanofibers layer. The results indicated that nanofiber addition enhanced filtration efficiency against very small particles (10–30 nm).

The electrospinning method allows us to produce fibers of any size [9,16]. However, the fabrication of ultrathin structures with diameters of ≈100 nm, especially uniform and beaded-free, is difficult [17]. The presence of beads is considered unfavorable and may disturb the filter operation [18]. The bead structures are formed due to the rivalry between electrical stress and capillary forces, which leads to electrohydrodynamic instabilities [17]. As the stretching of the electrospinning jet is dependent on the solution conductivity, it is possible to add some ionizable substances to enhance the stability of the polymer jet and to fabricate thin fibers [17,19]. Moreover, the added substances are not always safe for human health and may stay in the final products [18].

Some studies have shown that, among numerous polymers, poly(acrylonitrile) (PAN) is often used as the solution component in the electrospinning process. In the work in [20], PAN fibers were electrospun from dimethylformamide (DMF). By varying the parameters, such as polymer concentration, feed rate, and applied voltage, fibers with different sizes were produced. The authors received straight and beaded structures. The beads appeared when the fiber diameter was ≤350 nm. Cao and coauthors [18] fabricated poly(acrylonitrile) beaded-free nonwovens with fibers at a diameter of 77 nm. The parameters involved in fiber production referred to process temperature, solution concentration, applied voltage, collector rotation speed, tip-to-collector distance, and solution feed rate. The design of experiment (DOE) was used to upgrade the electrospinning process. Obtained structures was tested against cigarette smoke and particles released during 3D printing. Filtration efficiency was 99.26% in the first case and 99.26% in the second one.

Through the control of ambient humidity as well as the spinning solution concentration, the bead-on-string PAN structures were produced by Huang et al. [21]. The best filtration efficiency was 99%, with a pressure drop of 27 Pa. The multilayered PAN structure of fibers at ≈850 nm and ≈15,000 nm in diameter were fabricated by Liu et al. [16]; a 99.99% filtration efficiency at a pressure drop of 35 Pa was achieved. A 99.999% filtration efficiency against particles of 300 nm was obtained when using polyethersulfone/polyamide 66 membrane (PES/PA66); the average fiber diameter of the considered yarn was 520 nm [22].

A large number of different factors, incomplete reporting of the electrospinning process conditions, and limited knowledge about the role of these parameters make it difficult to obtain nonwovens of the desired structure. Therefore, it appears necessary to provide an appropriate, accurate mathematical model able to explain the system behavior with various components' influences. The nonlinear algebraic [23,24], differential, and differential-algebraic [25] models have been commonly used in the literature; usually, the (i) stable jet portion, (ii) whipping instability, or (iii) entire jet models are considered [19,26].

The axial length scale χ stands as an example of criterion for which the systematical calculation method has not been clearly investigated [23,24]. The main goal of this work is (i) to estimate the axial length scale with respect to specified experiment conditions of poly(acrylonitrile) electrospinning and (ii) to analyze how this parameter may leads to the nonwovens of fibers at certain sizes and functionalities (able to collect fine particulate matter fractions ($PM_{2.5}$)).

2. Methods

2.1. Mathematical Model

In this section, the performed methodology is described. The research was conducted using model (1) of a charged polymer solution jet at the terminal whipping stage [23,24], which is as follows:

$$F_D = C^{0.5}(\gamma\varepsilon\frac{Q^2}{I^2}\frac{2}{\pi(2\ln\chi - 3)})^{1/3}, \quad (1)$$

where F_D—fiber diameter (m), C —polymer solution concentration (wt %), γ —surface tension (N/m), ε —outside medium permittivity (A^2s^4/kgm^3), Q —flow rate (m^3/s), I — electric current (A), and χ—axial length scale. Moreover, according to the work of [17], it was assumed that

$$I \sim EQ^{0.5}K^{0.4}, \quad (2)$$

where E—electric field (V/m) and K—solution conductivity (S/m).

Model (1) is a function of the material and processing parameters and allows us to determine the final fiber size F_D of yarns produced via the electrospinning method.

2.2. Optimization Task

Based on model (1), the following nonlinear optimization task (3) was proposed:

$$\min_{\chi_n}\left(F_{Dn} - {C_n}^{0.5}\left(\gamma_n\varepsilon\frac{{Q_n}^2}{{I_n}^2}\frac{2}{\pi(2\ln\chi_n - 3)}\right)^{\frac{1}{3}}\right)^2 \quad (3)$$

where n—experiment number; $n = 1, \ldots, 42$ (Table 1); F_{Dn}—PAN fiber diameter (m); C_n — PAN/DMF solution concentration (wt %); γ_n—surface tension (N/m); ε —outside medium permittivity (A^2s^4/kgm^3); Q_n —flow rate (m^3/s); I_n —electric current (A); and χ_n—axial length scale.

It was assumed that the spinning solution was a mixture of poly(acrylonitrile) (PAN) and N,N-Dimethylformamide (DMF). The lower and upper bound inequality constraints for the unknown decision variable were introduced to ensure failure free computations:

$$4.5 \le \chi_n \le 6.70 \times 10^5. \quad (4)$$

The optimization task (3) was solved using the quasi-Newton's method (*fmincon* numerical optimization procedure, MATLAB computational environment). In general, the Newton's method is characterized by a fast (quadratic or superlinear) rate of convergence to the optimum. Nevertheless, the particular experiment settings may have a negative impact on the speed of the obtaining solution, e.g., a sharp slope effect can be observed. It should be noted that the considered problem is one-dimensional. Therefore, the amount of performed calculations depends directly on the number of test examples; MATLAB provides an approximated solution of the considered task, but the calculations were terminated according to the conditions related to the absolute values of the decision variable, objective function, as well as its first derivative. The applied Broyden–Fletcher–Goldfarb–Shanno (BFGS) method for calculating the second derivative guaranteed that the obtained solution was the local minimum. It is worth noting that other calculation procedures, such as metaheuristic or combined metaheuristic and stochastic algorithms, can be applied to solve the presented optimization approach.

Table 1. Fiber diameter (experiment and model).

No	Sample	Fiber Diameter (nm)		χ	APE (%)
		Experiment	Model		
1	S-05.1-13	50	76	6.70×10^{5}	51
2	S-05.1-16	50	66	6.70×10^{5}	32
3	S-05.1-22	50	53	6.70×10^{5}	7
4	S-05.1-25	60	60	2896	2
5	S-05.1-27	80	80	46.5	9
6	S-09.6-13	100	100	2374	6.60×10^{-7}
7	S-09.6-16	80	80	14579	3.80×10^{-7}
8	S-09.6-22	70	70	2658	3.20×10^{-7}
9	S-09.6-25	100	100	24.4	2.60×10^{-6}
10	S-09.6-27	100	100	19.2	3.60×10^{-7}
11	S-13.8-13	160	160	22.8	1.80×10^{-7}
12	S-13.8-16	120	120	57.3	3.80×10^{-8}
13	S-13.8-22	150	150	8.9	3.80×10^{-7}
14	S-13.8-25	130	130	10.2	1.40×10^{-7}
15	S-13.8-27	130	130	9	4.70×10^{-7}
16	S-16.1-13	190	190	11.6	1.00×10^{-6}
17	S-16.1-16	230	230	6.4	1.70×10^{-8}
18	S-16.1-22	170	170	7.1	7.50×10^{-7}
19	S-16.1-25	240	240	5.1	1.40×10^{-6}
20	S-16.1-27	240	240	5	1.60×10^{-6}
21	S-17.5-13	350	350	5.2	2.10×10^{-6}
22	S-17.5-16	400	400	4.8	1.00×10^{-5}
23	S-17.5-22	370	370	4.7	1.60×10^{-7}
24	S-17.5-25	380	380	4.6	1.80×10^{-6}
25	S-17.5-27	450	450	4.5	7.30×10^{-6}
26	S-19.0-13	450	450	4.9	2.00×10^{-6}
27	S-19.0-16	500	500	4.7	5.20×10^{-6}
28	S-19.0-22	590	590	4.5	1.80×10^{-5}
29	S-19.0-25	400	400	4.6	6.30×10^{-6}
30	S-19.0-27	600	600	4.5	2.80×10^{-5}
31	S-19.7-13	770	770	4.6	1.40×10^{-5}
32	S-19.7-16	800	800	4.5	4.50×10^{-6}
33	S-19.7-22	660	660	4.5	1.70×10^{-5}
34	S-19.7-25	760	760	4.5	8.30×10^{-6}
35	S-19.7-27	800	800	4.5	2.10×10^{-5}
36	S-20.3-13	900	900	4.5	2.30×10^{-5}
37	S-20.3-16	1200	1200	4.5	8.00×10^{-5}
38	S-20.3-22	1100	1100	4.5	1.20×10^{-4}
39	S-20.3-25	1000	1000	4.5	1.10×10^{-4}
40	S-20.3-27	1200	1004	4.5	16
41 *	S-08.0-16	82	105	6.70×10^{5}	28.27
42 **	S-11.0-12	340	340	6.35	7.90×10^{-7}

Test no. 1–40: $Q_{1,\ldots,40} = 1$ mL/h, $z_{1,\ldots,40} = 10$ cm; * Test no. 41: $Q_{41} = 1.6$ mL/h, $z_{41} = 15$ cm; ** Test no. 42: $Q_{42} = 0.8$ mL/h, $z_{42} = 15$ cm.

2.3. Simulation Research

In the next step, some simulations were carried out to obtain the desired fiber diameter of the PAN nonwovens. The analysis was performed for 10 different situations with respect to the parameters presented in Tables 2 and 3.

Table 2. Simulation parameters (case 1).

PAN solution concentration	$C_{41} = 8$	wt%	
flow rate	$Q_{41} = 1.6$	mL/h	
tip-to-collector distance	$z_{41} = 15$	cm	
applied voltage	$\Delta V_{41} = 16$	kV	
and	$\Delta V_{41a-41d} = \{12,\ 22,\ 25\ ,\ 27\}$	kV	respectively;

Table 3. Simulation parameters (case 2).

PAN solution concentration	$C_{42} = 11$	wt%	
flow rate	$Q_{42} = 0.8$	mL/h	
tip-to-collector distance	$z_{42} = 15$	cm	
applied voltage	$\Delta V_{42} = 12$	kV	
and	$\Delta V_{42a-42d} = \{16,\ 22,\ 25\ ,\ 27\}$	kV	respectively;

The results of simulations were collected and shown in Figures 1–6.

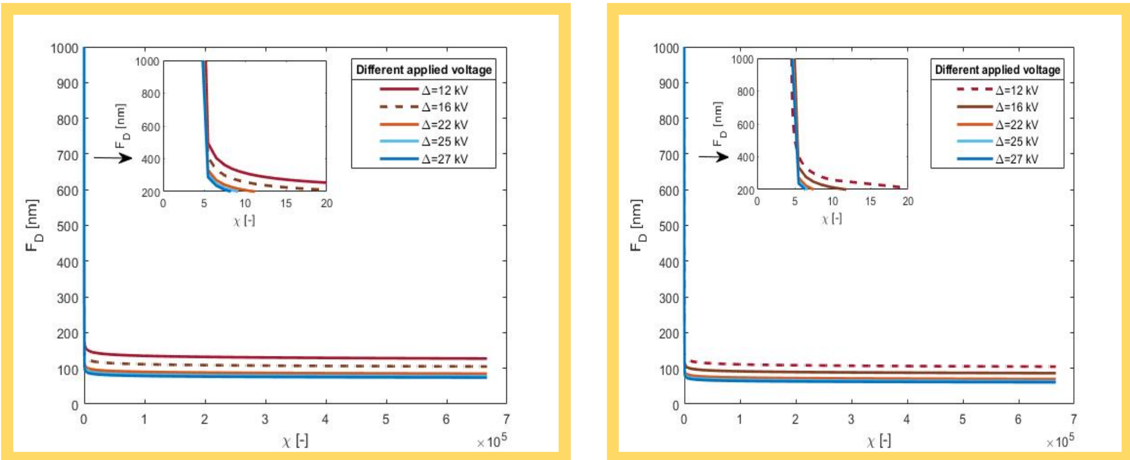

(**a**) (**b**)

Figure 1. The fiber diameter and characteristic axial length scale dependence: (**a**) 8 wt% of the poly(acrylonitrile) (PAN) solution and (**b**) 11 wt% of the PAN solution.

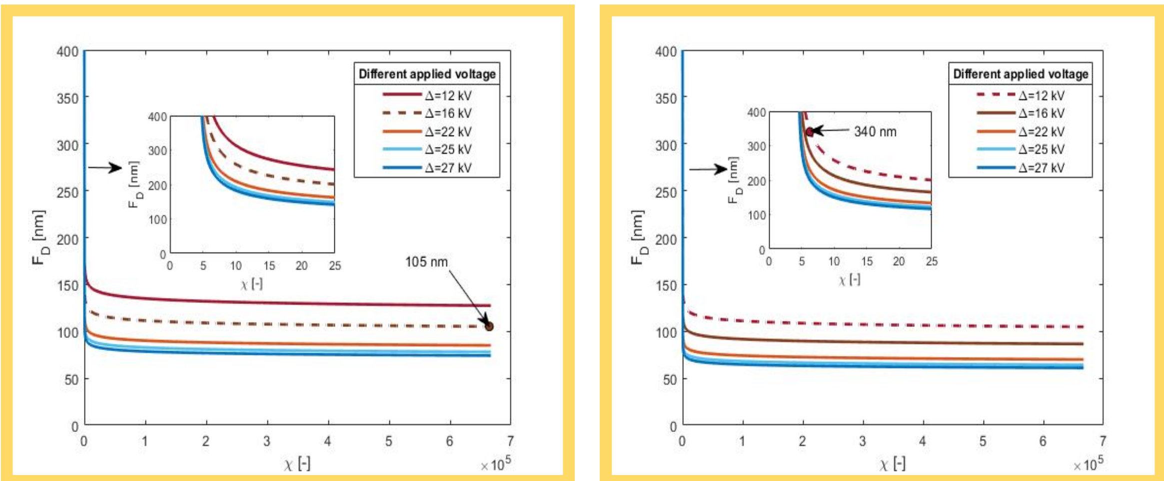

(**a**) (**b**)

Figure 2. The fiber diameter and characteristic axial length scale dependence: (**a**) 8 wt% of the poly(acrylonitrile) (PAN) solution and (**b**) 11 wt% of the PAN solution.

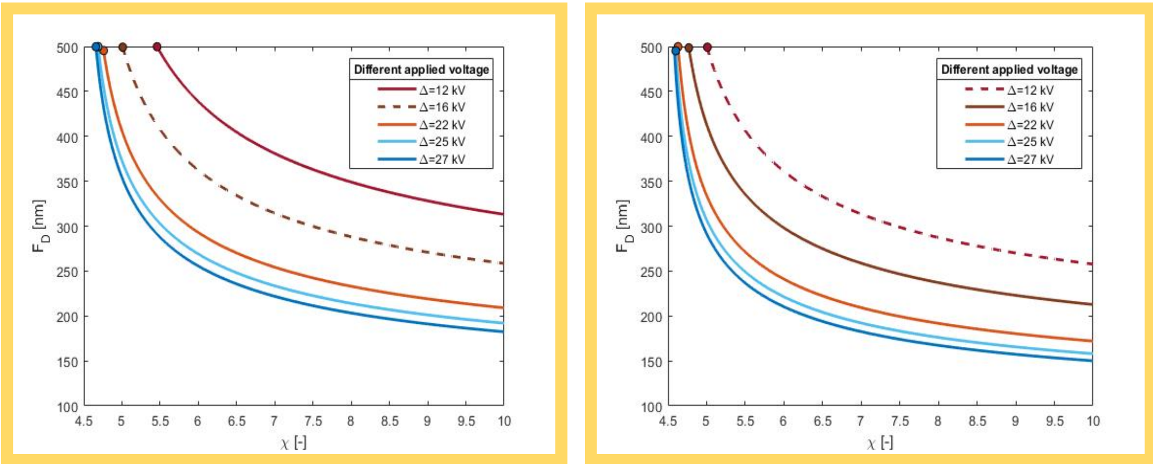

(**a**) (**b**)

Figure 3. The fiber diameter and characteristic axial length scale dependence: (**a**) 8 wt% of the poly(acrylonitrile) (PAN) solution and (**b**) 11 wt% of the PAN solution.

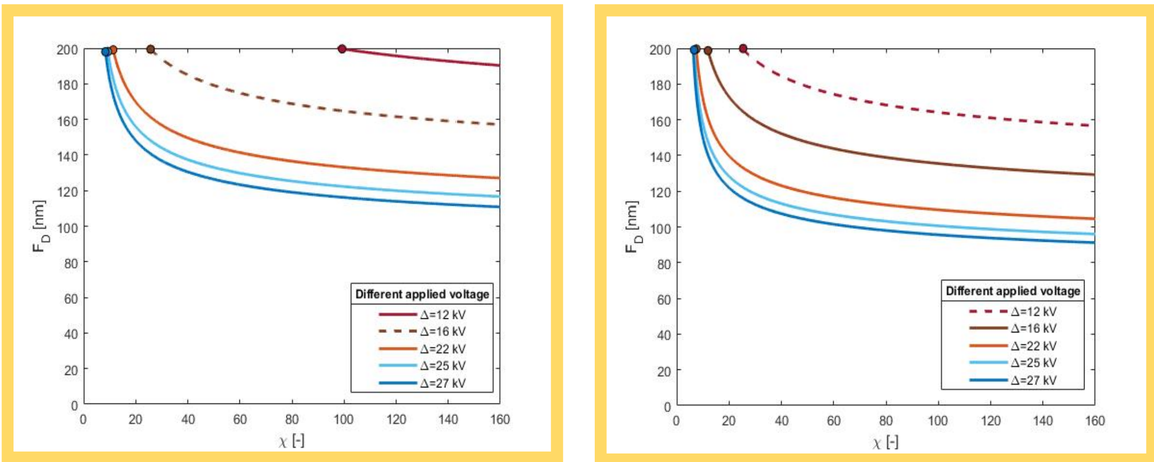

(**a**) (**b**)

Figure 4. The fiber diameter and characteristic axial length scale dependence: (**a**) 8 wt% of the poly(acrylonitrile) (PAN) solution and (**b**) 11 wt% of the PAN solution.

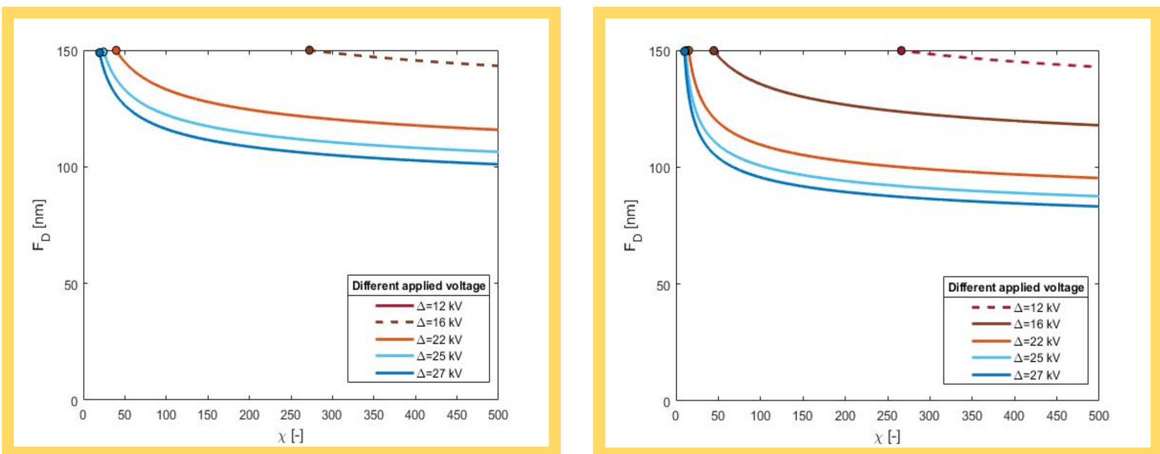

(**a**) (**b**)

Figure 5. The fiber diameter and characteristic axial length scale dependence: (**a**) 8 wt% of the poly(acrylonitrile) (PAN) solution and (**b**) 11 wt% of the PAN solution.

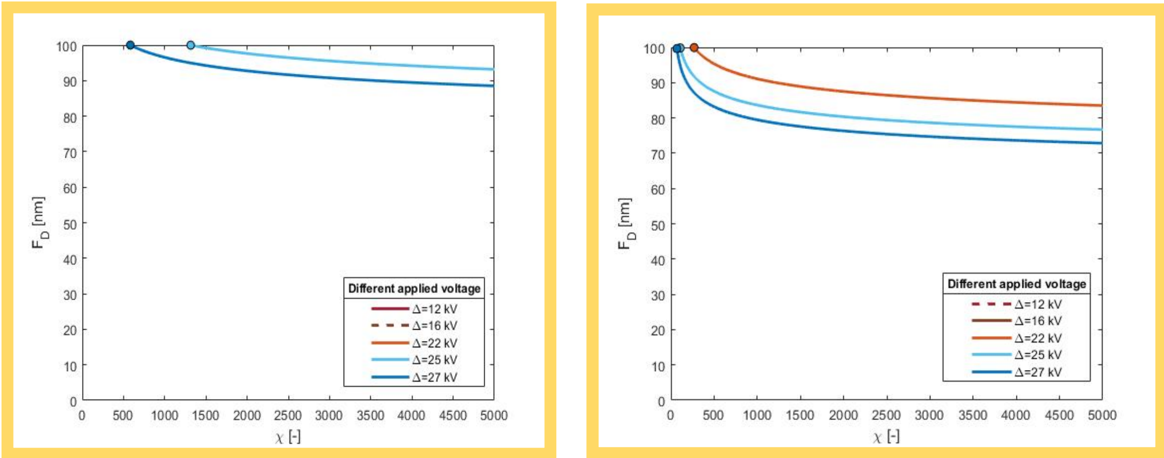

(**a**) (**b**)

Figure 6. The fiber diameter and characteristic axial length scale dependence: (**a**) 8 wt% of the poly(acrylonitrile) (PAN) solution and (**b**) 11 wt% of the PAN solution.

3. Model Validation

The mathematical model (1) was validated against experimental data [20,21]. To perform the model validation, the presented nonlinear optimization task (3) was solved. The absolute percentage error (APE) was used to measure model-experiment fitting accuracy:

$$\mathrm{APE} = \frac{|\mathrm{F_{DnE}} - \mathrm{F_{DnM}}|}{\mathrm{F_{DnE}}} \cdot 100\% \tag{5}$$

where $\mathrm{F_{DnE}}$—experimental PAN fiber diameter and $\mathrm{F_{DnM}}$—modeled PAN fiber diameter.

The obtained results are presented in Table 1. The applied designations, e.g., S-05.1-13, should be understood as a sample of 5.1 wt% and applied voltage of 13 kV. The appeared discrepancies were very small, mainly in terms of the range $1.00 \times 10^{-8} - 1.00 \times 10^{-4}$; the mean value of APE was 3.46%. Larger disproportions were seen in the case of extreme concentrations (low: 5.1 wt% or high 20.3 wt%). Therefore, it can be observed that the model results showed a satisfactory agreement with the experimental data. Moreover, the lower the polymer concentration, the higher the value of the χ parameter.

4. Results and Discussion

The presented research investigated what range of fibers size can be expected for the considered sets of parameters and the wide range of χ. The results are shown in Figure 1a (case 1) and Figure 1b (case 2). It can be seen that, in two instances, it was possible to produce fibers of 1000 nm in diameter (and less). In the next step, it was checked how the χ changes may affect the fibers of 105 nm and 340 nm diameter (Figure 2a,b, dashed line). As shown in Figure 2a, the slight changes in the χ values still led to fibers of ≈105 nm. However, as the χ values decreased, the fiber sizes became larger. The results shown in Figure 2b indicated that small changes in the χ values significantly influenced the size of the fibers; $\chi = 6.35$ led to the fibers of 340 nm diameter, while $\chi = 25$ led to fibers of ≈200 nm diameter. It can also be observed that, in both cases, the change in applied voltage had a crucial influence on the fiber size. The results of the simulations confirmed the rule that, the higher the voltage applied to the solution, the thinner the fibers obtained [19].

The individual ranges of χ values that lead to fibers with diameters of 500 nm, 200 nm, 150 nm, and 100 nm are shown in Figures 3–6. According to the results, it was possible to obtain fibers of $\mathrm{F_D} = 500$ nm, when $\chi \in [4.7; 5.5]$ (Figure 3a) and $\chi \in [4.7; 5.0]$ (Figure 3b) for all considered situations ($\Delta V = \{12, 16, 22, 25, 27\}$ kV). With regard to Figure 4, it was possible to obtain fibers of 200 nm diameter, when $\chi \in [8; 100]$ (Figure 4a) and

$\chi \in [6;\ 25]$ (Figure 4b) (also for all considered situations, where $\Delta V = \{12,\ 16,\ 22,\ 25,\ 27\}$). Further investigations are shown in Figure 5; it can be seen that, to obtain the fibers with $F_D = 150$ nm, $\chi \in [19.6;\ 272]$ (Figure 5a) and $\chi \in [11;\ 267]$ (Figure 5b) had to be used. It is also worth noting that it was not possible to obtain fibers of $F_D = 150$ nm when $\Delta V = 12$ kV (Figure 5a). To obtain fibers of $F_D = 100$ nm, $\chi \in [587;\ 1283]$ (Figure 6a) and $\chi \in [43;\ 239]$ (Figure 6b) were applied. Nevertheless, the production of fibers with this diameter and χ range was possible only for higher applied voltages: $\Delta V = \{25, 27\}$ (Figure 6a) and $\Delta V = \{22, 25, 27\}$ (Figure 6b).

According to the studies carried out, it was possible to determine the poly(acrylonitrile) fiber size with respect to the χ values and applied sets of parameters. The presented approach can be useful in terms of the filtration materials design. In general, the nonwovens of ultrathin fibers at $\approx$100 nm can be used to remove particles of aerodynamic diameter about 2500 nm or less. The nonwovens consisting of thick ($\approx$1000 nm) fibers can be used to remove bigger particles (aerodynamic diameter $\approx$10,000 nm). It is also possible to use hybrid solutions or constructions that can increase the packing density of the nonwovens (bead-on-string structures); the schematic view of fiber fabrication via electrospinning as well as the PM_{10} and $PM_{2.5}$ removing operations can be seen in Figures 7 and 8.

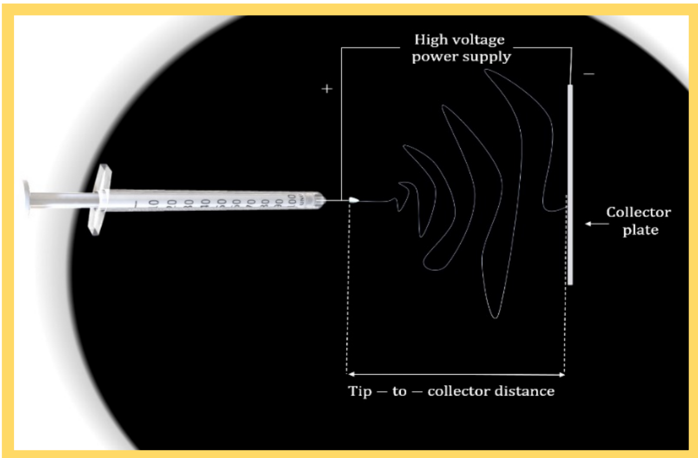

Figure 7. The schematic view of the nonwoven fabrication process via electrospinning.

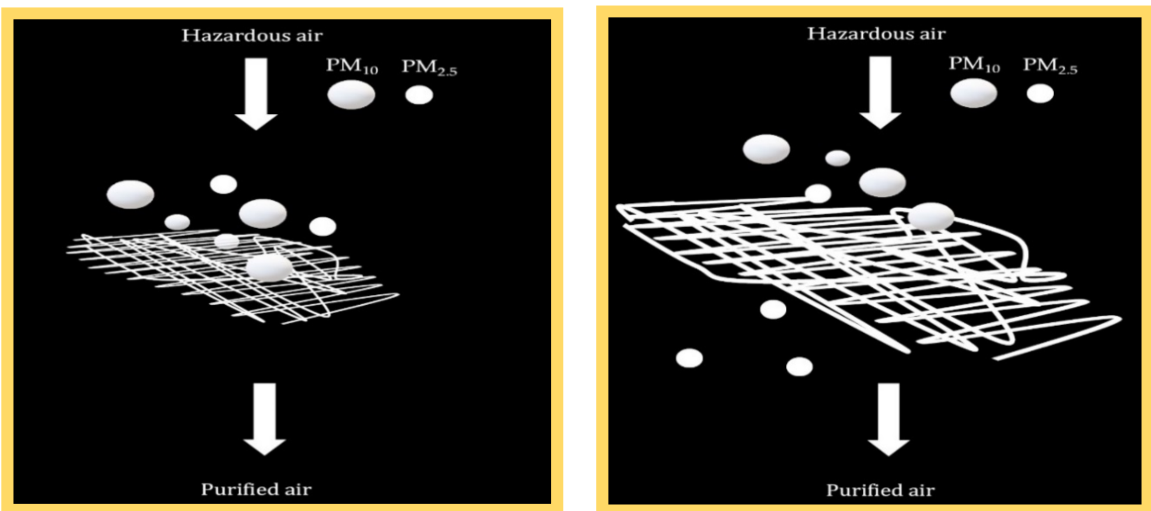

(**a**) (**b**)

Figure 8. *Cont.*

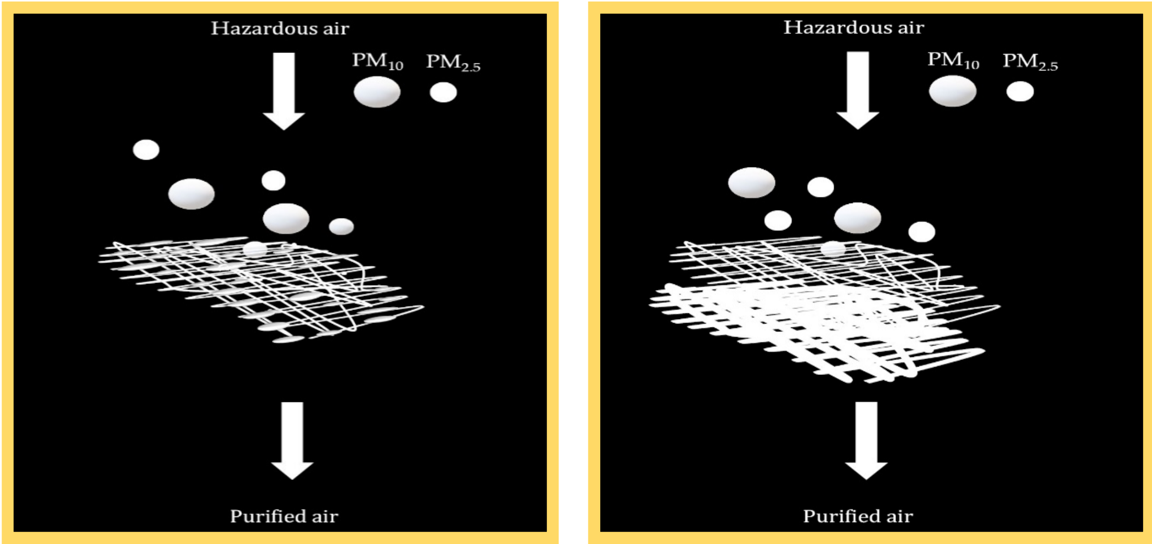

Figure 8. The schematic view of the PM_{10} and $PM_{2.5}$ removing processes: (**a**) electrospun nonwoven with ultrathin fibers, (**b**) electrospun nonwoven with thick fibers, (**c**) bead-on-string electrospun structure with ultrathin fibers, and (**d**) hybrid electrospun structure of ultrathin and thick fibers.

5. Conclusions

This study presented an estimation approach of the axial length scale χ; the investigated methodology was based on an analytical model of the charged poly(acrylonitrile) solution jet at the terminal whipping mode. It was established that the individual ranges of χ that lead to fibers with certain diameters took the following values with respect to the parameter sets considered in this work:

- $F_D = 500$ nm, when
  $\chi \in [4.7;\ 5.5]$ (case 1) and $\chi \in [4.7;\ 5.0]$ (case 2);
  $\Delta V = \{12,\ 16,\ 22,\ 25,\ 27\}$ kV;
- $F_D = 200$ nm, when
  $\chi \in [8;\ 100]$ (case 1) and $\chi \in [6;\ 25]$ (case 2);
  $\Delta V = \{12,\ 16,\ 22,\ 25,\ 27\}$;
- $F_D = 150$ nm, when
  $\chi \in [19.6;\ 272]$ and $\Delta V = \{16,\ 22,\ 25,\ 27\}$ (case 1);
  $\chi \in [11;\ 267]$ and $\Delta V = \{12,\ 16,\ 22,\ 25,\ 27\}$ (case 2);
- $F_D = 100$ nm, when
  $\chi \in [587;\ 1283]$ and $\Delta V = \{25,\ 27\}$ (case 1);
  $\chi \in [43;\ 239]$ and $\Delta V = \{22,\ 25,\ 27\}$ (case 2).

As urgent development of progressive solutions and technologies for Heating, Ventilation and Air-Conditioning filtration systems is needed, this research may be useful with regard to certain material designs for $PM_{2.5}$ removal (nonwovens consisting of ultrathin fibers, bead-on-string structures, or thin-thick fibers arrangements). The presented approach may be limited by the polymer-solution system properties and processing conditions. Thus, in a future work, it is also worth examining the role of the viscous force and determining in which situations it cannot be neglected.

Funding: This research was funded by the Department of Control Systems and Mechatronics at Wrocław University of Science and Technology.

Data Availability Statement: The data presented in this study are available in references [20,21].

Acknowledgments: The author would like to thank the anonymous reviewers for thoroughly reading the manuscript and for providing valuable comments.

Conflicts of Interest: The founders had no role in the design of the study; in the collection, analyses, or interpretation of data; in the writing of the manuscript; or in the decision to publish the results.

References

1. Wang, H.; Mullahy, J. Willingness to pay for reducing fatal risk by improving air quality: A contingent valuation study in Chongqing, China. *Sci. Total Environ.* **2006**, *367*, 50–57. [CrossRef]
2. Hao, Y.; Zheng Sh Zhao, M.; Wu, H.; Guo, Y.; Li, Y. Reexamining the relationships among urbanization, industrial structure, and environmental pollution in China—New evidence using the dynamic threshold panel model. *Energy Rep.* **2020**, *6*, 28–39.
3. Parviainen, A.; Casares-Porcel, M.; Marchesi, C.; Garrido, C.J. Lichens as a spatial record of metal air pollution in the industrialized city of Huelva (SW Spain). *Environ. Pollut.* **2019**, *253*, 918–929. [PubMed]
4. Chen, F.; Chen, Z. Cost of economic growth: Air pollution and health expenditure. *Sci. Total Environ.* **2021**, *755*, 142543. [CrossRef] [PubMed]
5. Zhuangbo, F.; Cao, S.H.-J. A newly developed electrostatic enhanced pleated air filters towards the improvement of energy and filtration efficiency. *Sustain. Cities Soc.* **2019**, *49*, 101569.
6. Tang, M.; Chen, S.-C.; Chang, D.-Q.; Xie, X.; Sun, J.; Pui, Y.H.D. Filtration efficiency and loading characteristics of $PM_{2.5}$ through composite filter media consisting of commercial HVAC electret media and nanofiber layer. *Sep. Purif. Technol.* **2018**, *198*, 137–145. [CrossRef]
7. Viegi, G.; Baldacci, S.; Maio, S.; Simoni, M. Indoor Air Pollution in Industrialized Countries. In *Reference Module in Biomedical Sciences*; Elsevier: Amsterdam, The Netherlands, 2019.
8. Zhang, Y.; Yuan Sh Feng, X.; Li, H.; Zhou, J.; Wang, B. Preparation of Nanofibrous Metal−Organic Framework Filters for Efficient Air Pollution Control. *J. Am. Chem. Soc.* **2016**, *138*, 5785–5788. [CrossRef]
9. Zhang, Q.; Li, Q.; Zhang, L.; Wang, S.; Harper, D.P.; Wu, Q.; Young, T.M. Preparation of electrospun nanofibrous poly(vinyl alcohol)/cellulose nanocrystals air filter for efficient particulate matter removal with repetitive usage capability via facile heat treatment. *Chem. Eng. J.* **2020**, *399*, 125768. [CrossRef]
10. Cui, J.; Tao, L.; Li, F.; Wang, Y.; Lei, J.; Ma, W.; Zou, Y.; Huang, C. Flexible and transparent composite nanofibre membrane that was fabricated via a "green" electrospinning method for efficient particulate matter 2.5 capture. *J. Colloid Interface Sci.* **2021**, *582*, 506–514. [CrossRef]
11. Lee, K.-S.; Hasolli, N.; Lee, J.R.; Kim, K.D.; Kim, S.D.; Park, Y.-O.; Hwang, J. Dust loading performance of a non-electret HVAC filter module in the presence of an external electric field. *Sep. Purif. Technol.* **2020**, *250*, 117204. [CrossRef]
12. Tang, M.; Thompson, D.; Chang, D.-Q.; Chen, S.-C.; Pui, D. Filtration efficiency and loading characteristics of $PM_{2.5}$ through commercial electret filter media. *Sep. Purif. Technol.* **2018**, *195*, 101–109. [CrossRef]
13. Cai, R.R.; Li, S.Z.; Zhang, L.Z.; Lei, Y. Fabrication and performance of a stable micro/nano composite electret filter for effective $PM_{2.5}$ capture. *Sci. Total Environ.* **2020**, *725*, 138297. [CrossRef] [PubMed]
14. Li, X.; Wang, N.; Fan, G.; Yu, J.; Gao, J.; Sun, G.; Ding, B. Electreted polyetherimide–silica fibrous membranes for enhanced filtration of fine particles. *J. Colloid Interface Sci.* **2015**, *439*, 12–20. [CrossRef] [PubMed]
15. Tang, M.; Thompson, D.; Chen, S.-C.; Liang, Y.; Pui, D. Evaluation of different discharging methods on HVAC electret filter media. *Build. Environ.* **2018**, *141*, 206–214. [CrossRef]
16. Liu, Y.; Qian, X.; Zhang, H.; Wang, L.; Zou, C.; Cui, Y. Preparing micro/nano-fibrous filters for effective $PM_{2.5}$ under low filtration resistance. *Chem. Eng. Sci.* **2020**, *217*, 115523. [CrossRef]
17. Balgis, R.; Kartikowati, C.W.; Ogi, T.; Gradon, L.; Bao, L.; Seki, K.; Okuyama, K. Synthesis and evaluation of straight and bead-free nanofibers for improved aerosol filtration. *Chem. Eng. Sci.* **2015**, *137*, 947–954. [CrossRef]
18. Cao, M.; Gu, F.; Rao Ch Fu, J.; Zhao, P. Improving the electrospinning process of fabricating nanofibrous membranes to filter $PM_{2.5}$. *Sci. Total Environ.* **2019**, *666*, 1011–1021. [CrossRef]
19. Ramakrishna, S.; Fujihara, K.; Teo, W.-E.; Lim, T.-C.; Ma, Z. *An Introduction to Electrospinning and Nanofibers*; World Scientific: Singapore, 2005.
20. Wang, T.; Kumar, S. Electrospinning of Polyacrylonitrile Nanofibers. *J. Appl. Polym. Sci.* **2006**, *102*, 1023–1029. [CrossRef]
21. Huang, J.J.; Tian, Y.; Wang, R.; Tian, M.; Liao, Y. Fabrication of bead-on-string polyacrylonitrile nanofibrous air filters with superior filtration efficiency and ultralow pressure drop. *Sep. Purif. Technol.* **2020**, *237*, 116377. [CrossRef]
22. Cao, J.; Cheng, Z.; Kang, L.; Zhang, Y.; Zhao, X.; Zhao, S.H.; Gao, B. Novel anti-fouling polyethersulfone/polyamide 66 membrane preparation for air filtration by electrospinning. *Mater. Lett.* **2017**, *192*, 12–16. [CrossRef]
23. Ismail, N.; Maksoud, F.J.; Ghaddar, N.; Ghali, K.; Tehrani-Bagha, A. Simplified modeling of the electrospinning process from the stable jet region to the unstable region for predicting the final nanofiber diameter. *J. Appl. Polym. Sci.* **2016**, *133*. [CrossRef]
24. Ismail, N.; Maksoud, F.J.; Ghaddar, N.K.; Ghali, T.-B.A. A mathematical model to predict the effect of electrospinning processing parameters on the morphological characteristic of nanofibrous web and associated filtration efficiency. *J. Aerosol Sci.* **2017**, *113*, 227–241. [CrossRef]

25. Drąg, M. The predictive differential-algebraic model for nano-fibrous webs production obtained via electrospinning method. In Proceedings of the 2019 20th International Carpathian Control Conference (ICCC), Kraków-Wieliczka, Poland, 26–29 May 2019; pp. 1–5.
26. Drąg, M.; Drąg, P. Model-based electrospinning process design for nanofibers production. In Proceedings of the XLVIII Seminar of Applied Mathematics, Boguszów Gorce, Poland, 9–11 September 2018; pp. 1–6.